CROSSMATCH: CROSS-CLASSIFIER CONSISTENCY REGULARIZATION FOR OPEN-SET SINGLE DOMAIN GENERALIZATION

Anonymous authors
Paper under double-blind review

ABSTRACT

Single domain generalization (SDG) is a challenging scenario of domain generalization, where only one source domain is available to train the model. Typical SDG methods are based on the adversarial data augmentation strategy, which complements the diversity of source domain to learn a robust model. Existing SDG methods require the source and target domains to have the same label space. However, as target domains may contain novel categories unseen in source label space, this assumption is not practical in many real-world applications. In this paper, we propose a challenging and untouched problem: *Open-Set Single Domain Generalization* (OS-SDG), where target domains include unseen categories out of source label space. The goal of OS-SDG is to learn a model, with only one source domain, to classify a target sample with correct class if it belongs to source label space, or assign it to unknown classes. We design a *CrossMatch* approach to improve the performance of SDG methods on identifying unknown classes by leveraging a multi-binary classifier. CrossMatch generates auxiliary samples out of source label space by using an adversarial data augmentation strategy. We also adopt a consistency regularization on generated auxiliary samples between multi-binary classifiers and the model trained by SDG methods, to improve the model's capability on unknown class identification. Experimental results on benchmark datasets prove the effectiveness of CrossMatch on enhancing the performance of SDG methods in the OS-SDG setting.

1 INTRODUCTION

Deep neural networks have obtained remarkable success in many classification tasks (Sze et al., 2017), as they can learn discriminative feature representations from data. These achievements are strongly relied on the independent and identically distributed (i.i.d) assumption (Vapnik, 1992), i.e., the training and test samples are from the same distribution. However, in real-world application, the i.i.d assumption is often violated due to the dataset shift problem. As a result, the performance of deep neural networks degrades notably (Hendrycks & Dietterich, 2019; Recht et al., 2019). To tackle this challenge, domain adaptation (DA) (Long et al., 2018; Peng et al., 2020) is proposed, which aims to mitigate the discrepancy between the source and target domains. DA assumes that both the source and target domains are accessible during model training. Even though DA has demonstrated promising performance on dealing with the dataset shift problem, it still fails in some practical scenarios when the target domains are unaccessible at the model training stage.

Domain generalization (DG) (Zhao et al., 2020b; Zhou et al., 2021b) is introduced to deal with the dataset shift problem and the absence of target domains. The goal of DG is to train a model from multiple source domains comprising the same label space, such that the learned model can generalize well to any unseen target domains. Despite of the success of DG in many real-world applications (Zhou et al., 2021a), it yet fails to a worst-case domain generalization scenario, single domain generalization (SDG). In SDG, only one source domain is available to train the model while the learned model need to generalize well on many unseen target domains. Several recent studies have made significant progress on this challenging yet practical scenario (Volpi et al., 2018; Zhao et al., 2020a; Qiao et al., 2020; Fan et al., 2021).

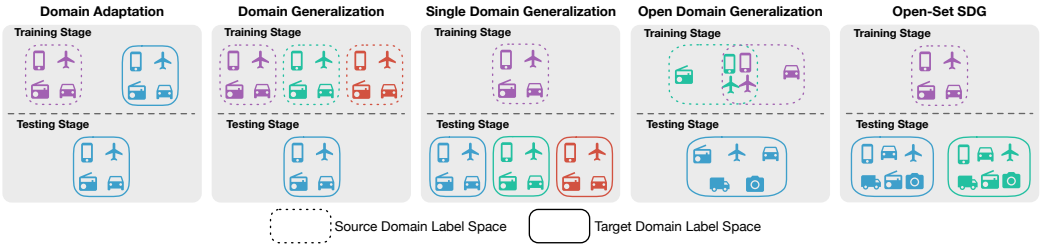

Figure 1: Illustration of label space of domain adaptation (DA), domain generalization (DG), single domain generalization (SDG), open domain generalization (ODG), and open-set single domain generalization (OS-SDG). Different colors represent different domains. As there is no prior knowledge about the target domains, existing DG and SDG methods cannot handle unknown classes (e.g., camera and truck) in target domain, which are unseen in source label space. ODG provides multiple source domains to learn a model. However, our proposed OS-SDG only supplies a single source domain, which is more challenging than ODG.

One assumption in DG and SDG is that the label spaces of source and target domains are uniform. However, in some more realistic scenarios such as autonomous driving and biomedical applications, it is possible that the target domains contain novel categories that are unseen in the source label space. As a result, the learned model cannot tackle target samples from novel categories, which dramatically degrades the robustness of existing DG and SDG methods. Until recently, this interesting yet tough problem is investigated by Shu et al. (2021), which proposes a task called open domain generalization (ODG). ODG assumes that both source and target domains have different label spaces, and multiple source domains are accessible for training. An ODG model either classifies a target sample with the correct class if it belongs to the multiple source label spaces, or marks it as unknown class.

In this paper, we consider a worst-case open-set problem (Geng et al., 2020) in SDG: only one source domain is accessible for training, and multiple target domains include samples that do not belong to any class in the source label space. We name this novel and challenging problem as *Open-Set Single Domain Generalization* (OS-SDG). Figure 1 illustrates the relationship between source and target label spaces in DA, DG, SDG, ODG, and OS-SDG. We also summarize how our problem is different from several related problems in Table 1. The goal of OS-SDG is to learn a model from a single source domain, which can generalize to unseen target domains with samples from unknown classes.

Inspired by universal domain adaptation (You et al., 2019; Saito et al., 2020), an "unknown" target sample tends to have a larger entropy of the learned model's output than samples from "known" classes. We can draw a boundary between "known" and "unknown" classes by using the entropy of the learned model's outputs. We evaluate the performance of representative SDG methods (Volpi et al., 2018; Zhao et al., 2020a) in the proposed OS-SDG task. Results (refer to Figure 5 in Section 4) show that the existing SDG methods have very limited capability on identifying unknown classes in target domains, although they obtain promising results in terms of per-class mean accuracy. These SDG methods only focus on synthesizing samples from diverse distributions to enrich source domain, and thus they cannot properly identify samples from unknown classes. The research challenge of modeling and identifying unknown classes in open-set single domain generalization is still untouched.

We propose a novel approach named *CrossMatch* to address the OS-SDG problem. First, CrossMatch induces unknown class information by generating auxiliary samples that are potentially out of the source label space. These auxiliary samples may not belong to the actual unknown classes in the target domains, as we do not have access to the target label space during training. However, we encourage the auxiliary samples to be far away from the known classes in the source domain, and thus they could still assist in identifying whether a sample belongs to known classes or not. In particular, we adopt a multi-binary classifier (Liu et al., 2019; Saito & Saenko, 2021) that consists of multiple one-vs-all binary classifiers. For a given sample, if all the binary classifiers mark it as negative, we believe this sample has a high probability of belonging to an unknown class. Therefore, this characteristic allows us to design a new loss function to generate auxiliary samples for unknown classes. Second, with the generated auxiliary samples for unknown classes, we minimize their entropy of multi-binary classifier's output to help model learn discriminative feature distributions between known and unknown classes, and improve the capability of multi-binary classifier on unknown class identification. Last, we design a novel consistency regularization to improve the capability of model on unknown class identification by propagating unknown class information, learned by multi-binary classifier, to the model.

Table 1: Illustration of difference between the proposed Open-Set Single Domain Generalization (OS-SDG) and other related tasks. $\mathcal{D}_s$ and $\mathcal{D}_t$ denote source and target domains, respectively. $\mathcal{C}_s$ and $\mathcal{C}_t$ denote the label space of source domain and target domain, respectively.

Task	More than one $\mathcal{D}_s$ for training ?	Need $\mathcal{C}_s = \mathcal{C}_t$?	Access to $\mathcal{D}_t$?
Domain Adaptation	×	✓	✓
Domain Generalization	✓	✓	×
Single Domain Generalization	×	✓	×
Open-Set Domain Adaptation	×	×	✓
Open Domain Generalization	✓	×	×
The Proposed OS-SDG	×	×	×

2 Related Work and Background

Domain Generalization (DG) aims to learn a model from multiple source domains and expect it to generalize over unseen target domains. Muandet et al. (2013) proposed a kernel-based method to learn domain invariant feature representations by minimizing the dissimilarity across source domains. Shankar et al. (2018) augment source domain by using adversarial gradients obtained from a domain discriminator. Zhou et al. (2020) synthesize samples by mapping source samples to pseudo-novel domains with an optimal transport-based distance measure. Recently, meta-learning has involved in DG problem (Li et al., 2018; Dou et al., 2019; Du et al., 2020). The main idea lies in learning the model under a domain shift which is induced by meta-train and meta-test from source domains.

Single Domain Generalization (SDG) is a more challenging and realistic problem than DG. It assumes the access to a labeled source domain $\mathcal{D}_s = \{(x_s^i, y_s^i)\}_{i=1}^{n_s}$ for training, and many unseen target domains $\mathcal{D}_t = \{\mathcal{D}_t^1, \ldots, \mathcal{D}_t^n\}$ for testing, where $\mathcal{D}_t^i = \{(x_{t,i}^j, y_{t,i}^j)\}_{j=1}^{n_t^i}$. The source and target domains are sampled from different distributions. We denote source and target label spaces as $\mathcal{C}_s$ and $\mathcal{C}_t$, respectively, where $\mathcal{C}_s = \mathcal{C}_t$. The goal of SDG is to learn a model from $\mathcal{D}_s$, which can generalize well on $\mathcal{D}_t$. Adversarial gradient-based augmentation is usually used in SDG for generating new samples to enrich the diversity of source domain. Firstly, Adversarial Data Augmentation (ADA) (Volpi et al., 2018) adopts sign-flipped gradients back-propagated from label classifier to generate new samples. Maximum-Entropy Adversarial Data Augmentation (MEADA) (Zhao et al., 2020a) further improves ADA by generating more "hard" samples. Qiao et al. (2020) use an auxiliary Wasserstein autoencoder to help ADA generate more "challenging" samples. Fan et al. (2021) design an adaptive normalization scheme with ADA to enhance the generalization of learned model.

Open-Set Recognition (OSR) aims to identifying unknown classes samples that are completely unseen during training process (Geng et al., 2020). Bendale & Boult (2016) propose a new model layer, i.e., OpenMax, to estimates the probability of a testing sample belongs to unknown class. Padhy et al. (2020) apply one-vs-all classifier to identify unknown class samples. Although many OSR methods have obtained significant achievement under a strong assumption that source and target domains have similar distribution, they still fails to address our proposed SS-SDG problem where source and target domains selected from different distribution.

Open-Set Domain Adaptation (OSDA) is proposed by Panareda Busto & Gall (2017) where both source domain and target domain have private label spaces, respectively, and the common label space is known. Recently, Saito et al. (2018) adjust the OSDA setting by claiming no source private label space, which means target label space contains source label space. Recent OSDA (Liu et al., 2019; Bucci et al., 2020) methods focus on this challenging setting. However, OSDA faces two limitations. First, it relies on an assumption that the target domain is accessible during training phase. Second, OSDA methods focus on the scenario that there are only one source domain and one target domain.

Open Domain Generalization (ODA) is proposed by (Shu et al., 2021). In this problem, a target domain and multiple source domains have different label spaces. The goal is to learn a model from multiple source domains to correctly classify each target sample into either a known class in the source label space or an unknown class. They utilize meta-learning framework to learn generalizable representations across domains augmented on both feature-level and label-level. Our OS-SDG problem is more challenging than the ODA problem and unsuitable for method in (Shu et al., 2021), as OS-SDG has only one source domain for training but multiple target domains for testing while ODA provides multiple source domains for training and one target domain for testing.

Worst-Case Problem is proposed by (Sinha et al., 2018). In single domain generalization, we consider to learn the model with source domain by solving the following objective function:

$$\min_{\theta} \sup_{\mathcal{D}_t} \left\{ \mathbb{E}[\mathcal{L}_{ce}(\theta; \mathcal{D}_s) : D(\mathcal{D}_t, \mathcal{D}_s) \leq \rho] \right\}, \tag{1}$$

where D represents a distance metric that measures the similarity between source and target domains. ρ indicates the largest transportation cost of moving $\mathcal{D}_s$ to $\mathcal{D}_t$. θ denotes model parameters optimized by cross-entropy loss function $\mathcal{L}_{ce}$.

Adversarial Data Augmentation (Volpi et al., 2018) aims to enrich the diversity of source domain by generating a domain $\mathcal{D}$ to approximate the unseen target domains $\mathcal{D}_t$. It reformulates worst-case problem (in Eq. 1) into a Lagrangian optimization problem with a fixed penalty parameter $\gamma \geq 0$:

$$\min_{\theta} \sup_{\mathcal{D}} \left\{ \mathbb{E}[\mathcal{L}_{ce}(\theta; \mathcal{D}_s)] - \gamma D(\mathcal{D}, \mathcal{D}_s) \right\}. \tag{2}$$

Here D denotes the Wasserstein metric (Volpi et al., 2018) used to preserve the semantics of the generated samples. The overall loss function is formulated as:

$$\mathcal{L}_{ada} = \mathcal{L}_{ce}(\theta; \mathcal{D}_s) - \gamma \mathcal{L}_{const}(\theta_g; \mathcal{D}, \mathcal{D}_s), \tag{3}$$

where $\mathcal{L}_{const}(\theta_g; \mathcal{D}, \mathcal{D}_s) = \|G(x) - G(x_s)\|_2^2 + \infty \cdot \mathbf{1}\{y \neq y_s\}$. The whole training process is an iterative procedure where two stages are alternated, i.e., maximization stage and minimization stage. At maximization stage, the new domain $\mathcal{D}$ is generated from $\mathcal{D}_s$ by maximizing $\mathcal{L}_{ada}$:

$$x_{t+1} \leftarrow x_t + \eta \nabla_{x_t} \mathcal{L}_{ada}(\theta; x_t). \tag{4}$$

After the maximization stage, the generated domain $\mathcal{D}$ is appended to $\mathcal{D}_s$. At the minimization stage, θ is optimized by minimizing the loss $\mathcal{L}_{ce}$ with $\mathcal{D}_s$.

Multi-Binary Classifier has proved its capability on unknown class identification in domain adaptation related problems (Liu et al., 2019; Saito & Saenko, 2021). A multi-binary classier F_b with k classes is defined as $F_b = \{F_b^1, \ldots, F_b^k\}$, where F_b^i is the i-th one-vs-all binary classifier with output $p_b^i = F_b^i(G(x)) \in \mathbb{R}^2$. We use $p_b^i(t = 0|x)$ and $p_b^i(t = 1|x)$, where $p_b^i(t = 0|x) + p_b^i(t = 1|x) = 1$, to indicate how likely the sample belongs to the i-th class and other classes, respectively. Recently, Saito & Saenko (2021) proposes a hard negative binary classifier sampling strategy for multi-binary classifier, which helps F_b learn a better boundary to identify unknown classes by minimizing the following loss function:

$$\mathcal{L}_{ova}(x, y) = -\log(p_b^y(t = 0|x)) - \min_{i \neq y} \log(1 - p_b^i(t = 1|x)). \tag{5}$$

Here the objective is to improve the robustness of multi-binary classifier on unknown class identification by optimizing each binary-classifier with the corresponding hard negative samples. Furthermore, for unlabeled samples, minimizing their multi-binary entropy loss $\mathcal{L}_{ent}^b$:

$$\mathcal{L}_{ent}^b(x) = -\sum_{i=1}^{k} p_b^i(t = 0|x) \log p_b^i(t = 0|x) + p_b^i(t = 1|x) \log p_b^i(t = 1|x). \tag{6}$$

They will either be aligned to source samples or be kept as unknown, and help improve the confidence of model on unknown class identification.

3 METHODOLOGY

In this section, we formally introduce the Open-Set Single Domain Generalization (OS-SDG) task, and then describe the proposed CrossMatch approach in detail.

3.1 OPEN-SET SINGLE DOMAIN GENERALIZATION

Given a labeled source domain $\mathcal{D}_s = \{(x_s^i, y_s^i)\}_{i=1}^{n_s}$ with label space $\mathcal{C}_s$, and multiple unseen target domains $\mathcal{D}_t = \{\mathcal{D}_t^1, \ldots, \mathcal{D}_t^n\}$ where $\mathcal{D}_t^i = \{(x_{t,i}^j, y_{t,i}^j)\}_{j=1}^{n_t^i}$ with label space $\mathcal{C}_t = \mathcal{C}_t^1 = \cdots = \mathcal{C}_t^n$. The source and target domains are sampled from different distributions. As target domains have novel classes that do not belong to $\mathcal{C}_s$, we denote those novel classes as an unknown class space in target

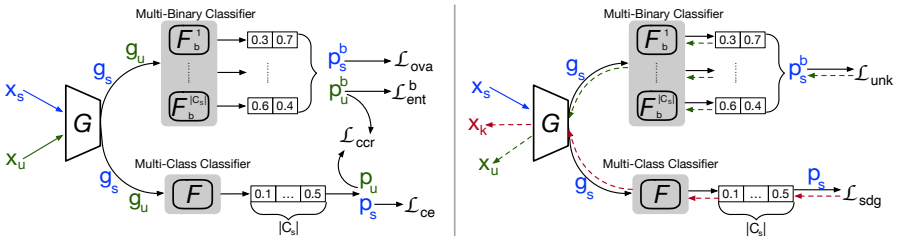

Figure 2: Overview of CrossMatch in SDG methods. x_s represents source samples while x_k and x_u denote generated known classes and auxiliary unkonwn classes samples, respectively. G is the feature extractor where $g_s = G(x_s)$. The multi-binary classifier is $F_b = \{F_b^1, \ldots, F_b^{|\mathcal{C}_s|}\}$ where $p_s^b = F_b(g_s)$. F is the multi-class classifier where $p_s = F(g_s)$. (a) At minimization stage, we adopt $\mathcal{L}_{ova}$(Eq. 5) and $\mathcal{L}_{ent}^b$ (Eq. 6) to optimize F_b while train F by cross-entropy loss $\mathcal{L}_{ce}$. We also propose a novel loss $\mathcal{L}_{ccr}$ to improve the capability of F on unknown class identification. (b) At maximization stage, SDG methods maximize their defined loss $\mathcal{L}_{sdg}$ to generate new samples to enrich the diversity of source domain in $\mathcal{C}_s$ while we propose an auxiliary sample generation loss $\mathcal{L}_{unk}$ to generate samples that far way from $\mathcal{C}_s$. After maximization stage, the generated x_k is appended to x_s and x_u is added to existed x_u.

domains, $\mathcal{C}_t^u = \mathcal{C}_t \backslash \mathcal{C}_s$. The goal of OS-SDG is to train a model with $\mathcal{D}_s$ to classify target samples into $|\mathcal{C}_s| + 1$ classes, where the novel classes in target domains are treated as one unknown class. Figure 1 illustrates the relationship of label space between source and target domains in OS-SDG. The research challenges in OS-SDG are twofold. First, how can we generate unknown classes samples that could complement sample diversity in the source domain? Second, what is an effective strategy to improve the model's capability on unknown class identification?

3.2 CROSSMATCH

The proposed CrossMatch approach generates auxiliary samples for unknown classes out of $\mathcal{C}_s$ (Sec. 3.2.1) and then exploits those samples to improve the capability of existing SDG methods on unknown class identification (Sec. 3.2.2). An overview of the proposed CrossMatch approach is shown in Figure 2.

Inspired by the worst-case problem defined in SDG, we extend it to OS-SDG setting based on the CrossMatch approach, as follows:

$$\min_{\theta, \theta_{f_b}} \sup_{\mathcal{D}=\{\mathcal{D}_k, \mathcal{D}_u\}} \{\mathbb{E}[\mathcal{L}_k(\theta, \theta_{f_b}; \mathcal{D}_s) + \mathcal{L}_u(\theta, \theta_{f_b}; \mathcal{D}_u) + \mathcal{L}_{unk}(\mathcal{D}_s)] : D(\mathcal{D}_k, \mathcal{D}_s) \leq \rho, D(\mathcal{D}_u, \mathcal{D}_s) \geq \rho\}, \tag{7}$$

where $\theta = \{\theta_g, \theta_f\}$ includes the parameters of feature extractor G and multi-class classifier F. θ_{f_b} is the parameters of multi-binary classifier F_b. $\mathcal{D} = \{\mathcal{D}_k, \mathcal{D}_u\}$ denotes the augmented domain consists of known classes domain $\mathcal{D}_k$ and auxiliary unknown classes domain $\mathcal{D}_u$. $\mathcal{L}_k = \{\mathcal{L}_{ce} + \mathcal{L}_{ova}\}$ represents those loss functions who use $\mathcal{D}_s$ to optimize model, i.e., cross-entropy loss $\mathcal{L}_{ce}(\theta_g, \theta_f; x_s)$ and one-vs-all loss $\mathcal{L}_{ova}(\theta_g, \theta_{f_b}; x_s)$ (in Eq. 5). $\mathcal{L}_u = \{\mathcal{L}_{ent}^b + \alpha \mathcal{L}_{ccr}\}$ indicates those loss functions who optimize model with $\mathcal{D}_u$, i.e., multi-binary entropy loss $\mathcal{L}_{ent}^b(\theta_g, \theta_{f_b}; x_u)$ (Eq. 6) and our proposed cross-classifier consistency regularization loss $\mathcal{L}_{ccr}(\theta_g, \theta_f, \theta_{f_b}; x_u)$ which improves the capability of F on unknown class identification by propagating unknown classes information, learned by F_b, to F. $\mathcal{L}_{unk}(\mathcal{D}_s)$ (Eq. 13) our proposed novel loss function for generating auxiliary samples. D is the Wasserstein metric and ρ is the largest domain discrepancy between two domains.

At minimization stage, the overall loss function is defined as follows:

$$\mathcal{L}_{min} = \mathcal{L}_{ce} + \mathcal{L}_{ova} + \mathcal{L}_{ent}^b + \alpha \mathcal{L}_{ccr}, \tag{8}$$

where α is the hyper-parameter.

At maximization stage, we aims to generate two kinds of samples: known classes samples $x_k \in \mathcal{D}_k$ and auxiliary samples $x_u \in \mathcal{D}_u$ which far away from the known classes in the source domain. For

known class samples, we consider the following Lagrangian relaxation derived from Eq. 7 with penalty parameter γ:

$$\min_{\theta} \sup_{\mathcal{D}_k} \left\{ \mathbb{E}[\mathcal{L}_{ce}(\theta; \mathcal{D}_s)] - \gamma D(\mathcal{D}_k, \mathcal{D}_s) \right\}, \tag{9}$$

where $D(\mathcal{D}_k, \mathcal{D}_s) = \mathcal{L}_{const}(\theta_g; \mathcal{D}_k, \mathcal{D}_s)$ defined in Eq. 3. To solve this penalty problem in Eq. 9, we adopt the same strategy in (Volpi et al., 2018) with the suitable conditions (Boyd et al., 2004) by performing stochastic gradient descent procedures. We define the robust surrogate loss $\phi(\theta; x_s, y_s) = \sup_{x_k \in \mathcal{D}_k} \{\mathcal{L}_{ce}(\theta; x_k, y_s) - \gamma \mathcal{L}_{const}(\theta_g; x_k, x_s)\}$ and have $\nabla_\theta \phi(\theta; x_s, y_s) = \nabla_\theta \mathcal{L}_{ce}(\theta; x_k^*, y_s)$, where $x_k^* = \arg\max_{x_k \in \mathcal{D}_k} \{\mathcal{L}_{ce}(\theta; x_k, y_s) - \gamma \mathcal{L}_{const}(\theta_g; x_k, x_s)\}$ is an adversarial perturbation of x_s at the current model θ. We adopt a few iterations to generate known class samples by:

$$x_k^{t+1} \leftarrow x_k^t + \eta \nabla_{x_k^t} \{\mathcal{L}_{ce}(\theta; x_k^t, y_s) - \gamma \mathcal{L}_{const}(\theta_g; x_k^t, x_s)\}. \tag{10}$$

Here the generation Eq. 10 is consistence with single domain generation method ADA (Volpi et al., 2018), it can be further extended to other single domain generation method, e.g., MEADA (Zhao et al., 2020a), by updating the loss $\mathcal{L}_{ce}$ with more items. Similar to the way of generating known class samples, we also convert Eq. 7 into a Lagrangian relaxation to generate auxiliary samples with penalty parameter γ:

$$\min_{\theta} \sup_{\mathcal{D}_u} \left\{ \mathbb{E}[\mathcal{L}_{unk}(\theta_g, \theta_{fb}; \mathcal{D}_s)] + \gamma D(\mathcal{D}_u, \mathcal{D}_s) \right\}. \tag{11}$$

By adopting the same strategy as known class sample generation process, we can generate auxiliary samples with a few iterations:

$$x_u^{t+1} \leftarrow x_u^t + \eta \nabla_{x_u^t} \{\mathcal{L}_{unk}(\theta_g, \theta_{fb}; x_u^t) + \gamma \mathcal{L}_{const}(\theta_g; x_u^t, x_s)\}, \tag{12}$$

where η is the learning rate of stochastic gradient ascent. The details of $\mathcal{L}_{unk}$ and $\mathcal{L}_{ccr}$ will be described in Section 3.2.1 and Section 3.2.2, respectively.

Remarks. CrossMatch aims to tackle the challenges in OS-SDG from two aspects: generation of auxiliary samples for unknown classes and improvement of unknown class identification. The key innovation of the proposed approach lies in jointly encouraging model to generate auxiliary samples for unknown classes by maximizing our new designed loss $\mathcal{L}_{unk}$ at maximization stage, and improving the capability of multi-class classifier F on unknown class identification by optimizing our proposed cross-classifier consistency regularization loss $\mathcal{L}_{ccr}$ with generated auxiliary samples for unknown classes at the minimization stage.

3.2.1 Auxiliary Sample Generation for Unknown Classes

The key idea of adversarial data augmentation is to use sign-flipped gradients back-propagated from a label classifier or other related terms (Volpi et al., 2018; Qiao et al., 2020) to generate diversified samples. Inspired by the structure of multi-binary classifier F_b, if a given sample is classified as 'other class' by all the binary classifiers in F_b, it has a high probability to be associated with unknown classes. For example, $\mathcal{C}_s$ contains four known classes (e.g., 'phone', 'airplane', 'radio' and 'car') and $\mathcal{C}_t^u$ consist of two unknown classes 'truck' and 'camera', as illustrated in Figure 1. We assume that F_b has been well trained in the source domain. If a target sample belongs to the class 'phone', the corresponding binary classifier should output a high probability to 'phone', while the other binary classifiers will classify it as 'other class'. But, if a target sample belongs to 'truck', all the binary classifiers would classify it as 'other class'.

With this insight, we design a novel auxiliary sample generalization loss $\mathcal{L}_{unk}$ to generate samples that are possibly out of source label space. Given a source sample x_s with label y_s, multi-binary classifier F_b and feature extractor G, we denote $\mathcal{L}_{unk}$ as:

$$\mathcal{L}_{unk}(x) = -\log(p_b^y(t=0|x)) + \sum_{i \neq y}^{k} \log p_b^i(t=1|x), \tag{13}$$

where $p_b^y(t=0|x)$ and $p_b^y(t=1|x)$ represent the probabilities of being y-th class and other classes from the y-th binary classifier, respectively. By maximizing $\mathcal{L}_{unk}$ at the maximization stage, it encourages the model to generate new samples that all binary classifiers in F_b predict it as other class. Thus, the new generated sample could belong to unknown classes. As entropy loss function has proved its effectiveness on diversifying the adversarial generated samples (Zhao et al., 2020a), we also add multi-binary loss $\mathcal{L}_{ent}^b$ to $\mathcal{L}_{unk}$.

3.2.2 CROSS-CLASSIFIER CONSISTENCY REGULARIZATION

With the generated auxiliary samples for unknown classes, we minimize the multi-binary entropy loss $\mathcal{L}_{ent}^{b}$ to enhance the capability of multi-binary classifier F_b on unknown class identification, and help feature extractor G learn discriminative feature representations to benefit multi-class classifier F on unknown class identification. Each auxiliary sample x_u will be aligned to source samples if it really belongs to $\mathcal{C}_s$, or kept as unknown. To make full use of unknown classes information learned by F_b, we propose the cross-classifier consistency regularization loss, termed as *cross-classifier consistency regularization* (CCR), to propagate those information learned by F_b to F. The key idea lies in encouraging F_b and F to produce the similar output distribution, in form of one-vs-all, for each generated auxiliary sample from $\mathcal{D}_u$:

$$\mathcal{L}_{ccr}(x) = \sum_{i=1}^{k} \left\| p_b^i - p_{b'}^i \right\|_2^2, \tag{14}$$

where $p_b^i \in \mathbb{R}^2$ represents the i-th binary classifier's output. $p_{b'}^i$ indicates the one-vs-all version of multi-class classifier F's output p, i.e., $p_{b'}^i = \left[p^i, 1 - p^i\right]$, p^i is the probability of x belongs to i-th class. Different from previous consistency regularization (Laine & Aila, 2017; Sajjadi et al., 2016), which encourages classifier to produce similar outputs for sample under different augmentations, our CCR encourages different classifiers to generate similar output distributions for given sample.

3.3 INFERENCE

Figure 3 illustrates the inference procedure where the learned model M consists of a feature extractor G and a multi-class classifier F. The target sample is marked as unknown class if its entropy is larger than the threshold μ. Otherwise, it will be assigned to a class in the source label space $\mathcal{C}_s$.

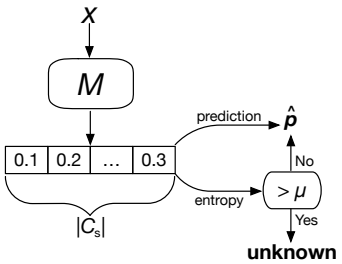

Figure 3: Inference procedure.

4 EXPERIMENTS

4.1 EXPERIMENTAL SETUP

We briefly introduce the experimental setup in this section. More details about the experimental settings and results on additional datasets are provided in the Appendix due to space limit.

Datasets. (1) ***Digits*** comprises of five digits datasets: **MNIST** (LeCun et al., 1989), **SVHN** (Netzer et al., 2011), **USPS** (Hull, 1994), **MNIST-M** and **SYN** (Ganin & Lempitsky, 2015). **MNIST** is the source domain, and its label space includes numbers from 0 to 4. The other datasets are treated as target domains, and their target unknown label space $\mathcal{C}_t^u$ contains numbers from 5 to 9. (2) ***Office31*** (Saenko et al., 2010) contains 31 classes collected from three visually distinct domains: **A**, **D** and **W**. The 10 classes shared by Office-31 and Caltech-256 (Gong et al., 2012) form the source label space $\mathcal{C}_s$. In alphabetical order, the last 11 classes are used as target unknown class space $\mathcal{C}_t^u$. Due to **D** and **W** are relatively small, we only use **A** as the source domain. (3) ***Office-Home*** (Venkateswara et al., 2017) consists of four domains: **Artistic**, **Clip Art**, **Product**, and **Real-World**. It comprises of 65 categories from four dissimilar domains. In alphabetic order, we select the first 15 classes as the source label space $\mathcal{C}_s$. The remaining 50 classes are viewed as target unknown label space $\mathcal{C}_t^u$. Each domain serves as source domain, and the rest are target domains. (4) **PACS** (Li et al., 2017) consists of four domains: Art Paint, Cartoon, Sketch, and Photo. It has 9,991 images from seven object categories.

Implementation Details. For ***Digits***, we adopt the ConvNet (LeCun et al., 1989) with architecture *conv-pool-conv-pool-fc-fc-softmax*, resize all images to 32×32, and follow the settings in Volpi et al. (2018); Zhao et al. (2020a). For ***Office31***, ***Office-Home*** and ***PACS***, we use an ImageNet-pretrained ResNet18 (He et al., 2016) as the base network.

Baselines and Metrics. We adopt the Empirical Risk Minimization (ERM) (Koltchinskii, 2011) as a simple baseline without any consideration of SDG. We compare with two state-of-the-art SDG methods, Adversarial Data Augmentation (ADA) (Volpi et al., 2018) and Maximum-Entropy Adversarial Data Augmentation (MEADA) (Zhao et al., 2020a). We also adopt Open Set Domain

Table 2: Results (%) on *Digits* (ConvNet) and *Office31* (ResNet18).

Dataset	Metric	OSDAP	OpenMax	ERM	+CM	ADA	+CM	MEADA	+CM
Digits	*acc*	41.42	42.38	49.17	49.07	50.22	49.71	52.98	51.27
	acc_u	70.60	83.81	13.04	**53.52**	15.11	**52.07**	29.83	**46.11**
	acc_s	35.59	34.40	56.40	48.67	57.24	49.24	57.61	52.30
	hs	40.46	40.67	17.97	**40.15**	20.14	**39.93**	30.37	**38.70**
Office31	*acc*	76.51	18.19	79.82	78.30	80.13	78.61	80.26	78.98
	acc_u	84.28	100.0	27.04	**37.60**	25.24	**34.51**	25.09	**41.08**
	acc_s	75.77	10.01	85.10	82.37	85.62	83.02	85.78	82.77
	hs	77.68	16.74	40.69	**51.14**	38.65	**48.50**	38.55	**54.69**

Table 3: Results (%) on *Office-Home* (ResNet18).

Method	Artistic		Clip Art		Product		Real-World		Average	
	acc	*hs*	*acc*	*hs*	*acc*	*hs*	*acc*	*hs*	*acc*	*hs*
OSDAP	45.61	52.35	52.78	58.82	41.45	47.95	53.51	58.40	48.34	54.38
OpenMax	22.42	30.64	22.67	29.51	15.10	16.65	25.54	33.07	21.43	27.47
ERM	65.00	31.07	64.12	35.78	60.53	36.33	66.59	33.92	64.06	34.28
ERM+CM	65.49	52.85	63.37	50.51	58.03	47.25	67.75	52.60	63.66	**50.80**
ADA	68.29	32.94	65.10	42.09	60.52	34.72	67.04	34.86	65.24	36.15
ADA+CM	66.30	46.68	62.64	49.31	58.72	47.47	66.82	50.47	63.62	**48.48**
MEADA	68.31	33.29	65.25	42.05	60.43	35.68	67.04	34.65	65.01	36.42
MEADA+CM	65.85	53.22	62.90	48.87	58.36	45.34	67.10	50.77	63.55	**49.55**

Adaptation by Backpropagation (OSDAP) (Saito et al., 2018) a representative method in open-set domain adaptation and OpenMax (Bendale & Boult, 2016) a typical open-set recognition method as baselines. Furthermore, we extend ERM, ADA, and MEADA using the proposed CrossMatch (CM) approach (denoted by "+CM"). We adopt the overall accuracy (acc), unknown class accuracy (acc_u) and *h-score* (*hs*) (Fu et al., 2020) as evaluation metrics.

4.2 Results and Discussions

***Digits* and *Office31*.** Table 2 shows the results of our approach and baselines on the *Digits* and *Office31* datasets in terms of mean accuracy (*acc*), unknown class accuracy (acc_u) and h-score (*hs*). ERM is a simple baseline without any consideration of adversarial data augmentation. Our proposed method is superior to ADA by more than 19% and 9% with respect to *hs* on *Digits* and *Office31*, respectively. Compared with the state-of-the-art method MEADA, which obtains the best *acc* among all the methods, our method still significantly outperforms it with more than 8% and 16% in terms of *hs* on *Digits* and *Office31*, respectively. Meanwhile, our method achieves comparable mean accuracy (*acc*) than baselines. The strong baseline method OSDAP, uses source and target domains to learn the model, gets better results with regard to acc_u in *Digits* and *Office31* datasets. While our method learns the model without target domain but gets similar performance in terms of hs in *Digits*, which proves the effectiveness of our method. Compared with representative open-set recognition method, OpenMax, our method obtains similar results in terms of hs and better performances with regard to acc and acc_s in *Digits* dataset. Due to domain shift problem, OpenMax gets high performance in terms of acc_u by marking most of testing samples as unknown class. When domain shift is larger in *Office31* dataset, we find that OpenMax get worse performance in terms of acc, acc_s, and hs.

***Office-Home*.** Table 3 shows the *acc* and *hs* on *Office-Home*. Each time, one domain serves as the source domain and the rest three ones are target domains. *Office-Home* is more challenging than the previous two datasets because it contains more target unknown classes than them. Although the performance of our method on *acc* is slightly lower than baselines, we observe remarkable improvement of 16.52%, 12.22%, and 13.13% compared with ERM, ADA, and MEADA in terms of *hs*, respectively. Such improvements over baselines demonstrate the effectiveness of our method. Furthermore, compared with strong baseline OSDAP, our method gets better performance in terms of acc and similar results on hs, demonstrates the efficiency of our method. OpenMax fails to correctly identify known classes due to significant domain shift existed in *Office-Home* dataset.

Table 4: Results (%) on *PACS* (ResNet18).

Method	Art Paint		Cartoon		Sketch		Photo		Average	
	acc	*hs*	*acc*	*hs*	*acc*	*hs*	*acc*	*hs*	*acc*	*hs*
OSDAP	53.30	46.58	43.73	38.81	42.05	41.03	30.81	32.89	42.47	39.83
OpenMax	52.59	53.60	31.71	25.23	29.85	19.87	27.60	19.47	35.44	29.54
ERM	62.24	38.90	55.34	40.96	39.19	28.89	38.32	35.74	48.77	36.12
ERM+CM	63.52	44.9	57.6	48.31	38.53	30.43	42.52	41.6	**50.54**	**41.31**
ADA	62.48	39.02	56.43	41.55	39.03	26.93	40.28	38.13	49.56	36.41
ADA+CM	64.26	42.4	60.41	51.81	42.48	35.18	43.97	42.76	**52.78**	**43.04**
MEADA	62.43	38.85	56.1	41.34	38.89	26.43	39.88	38.24	49.33	36.22
MEADA+CM	62.63	41.88	60.03	51.36	41.51	35.76	43.5	41.6	**51.92**	**42.65**

PACS. We further evaluate the effectiveness of our method on *PACS* dataset. As shown in Table 4, our method outperforms all the baselines in terms of acc and hs. In particular, our method significantly improve the capability of baselines, i.e., ERM, ADAN and MEADA, on unknown class identification while slightly enhance the averaged accuracy over all classes. For other two baselines, i.e., OSDAP and OpenMax, we observe the similar phenomenon as *Office-Home* where large domain gaps are existed among source and target domains.

4.3 Analysis

Table 5: Ablation study for loss items: $\mathcal{L}'_{unk}$, $\mathcal{L}_{unk}$, and $\mathcal{L}_{ccr}$ on *Digits* dataset.

$\mathcal{L}'_{unk}$	$\mathcal{L}_{unk}$	$\mathcal{L}_{ccr}$	acc	acc_u	hs
			52.98	29.83	30.37
✓			51.86	29.01	29.36
	✓		51.08	42.55	36.94
✓		✓	52.16	30.47	30.55
	✓	✓	51.27	46.11	38.70

On the Effect of $\mathcal{L}_{unk}$ and $\mathcal{L}_{ccr}$. We investigate the efficacy of the proposed $\mathcal{L}_{unk}$ (Eq. 13) and $\mathcal{L}_{ccr}$ (Eq. 14) on *Digits* datasets with MEADA method. To prove the advantage of $\mathcal{L}_{unk}$ on generating auxiliary samples for unknown classes, we compare it with a baseline $\mathcal{L}'_{unk} = \mathcal{L}_{ova} + \mathcal{L}^b_{ent}$. The major difference between $\mathcal{L}_{unk'}$ and $\mathcal{L}_{unk}$ is that the former aims to generate samples that are hard for F_b to separate, while the latter prefers to generate those out of $\mathcal{C}_s$. As shown in Table 5, the first row denotes the performance of MEADA. Firstly, comparing results in the first three rows, we find that our proposed $\mathcal{L}_{unk}$ outperforms $\mathcal{L}'_{unk}$ in terms of acc_u and hs, demonstrating the advantage of $\mathcal{L}_{unk}$ on generating auxiliary samples for unknown classes. Adding $\mathcal{L}'_{unk}$ to MEADA degrades the performance. Secondly, the performance of both $\mathcal{L}_{unk}$ and $\mathcal{L}'_{unk}$ are improved by adding $\mathcal{L}_{ccr}$, which validates the effectiveness of $\mathcal{L}_{ccr}$.

Varying Size of Common Label Space. To verify the robustness of our method under different sizes of source label space, we conduct experiments on *Office-Home* where *Real-World* is selected as the source domain. The size of common label space varies from 10 to 60. As shown in Figure 4, our method continuously outperforms MEADA with significant improvements under different sizes of common label space. In addition, our method obtains similar results as MEADA in terms of acc. It indicates that our method can improve the capability of single domain generalization methods on unknown class identification.

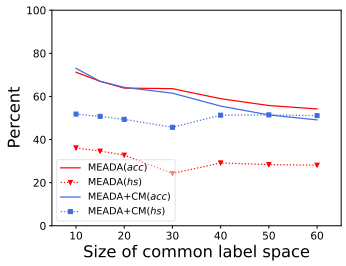

Figure 4: Varying the size of common label space.

5 Conclusion

In this paper, we propose a new domain generalization task, i.e., open-set single domain generalization (OS-SDG), which aims to generalize models from a single source domain to unseen target domains and simultaneously deals with unknown classes. We further propose a novel CrossMatch approach to tackle the OS-SDG task, which generates auxiliary samples for unknown classes and improves the capability of unknown classes identification with a novel consistency regularization. Extensive experiments demonstrate that the proposed CrossMatch method largely facilitates the capability of existing single domain generalization methods on unknown class identification.

REFERENCES

Abhijit Bendale and Terrance E Boult. Towards open set deep networks. In *CVPR*, pp. 1563–1572, 2016.

Stephen Boyd, Stephen P Boyd, and Lieven Vandenberghe. *Convex optimization*. Cambridge university press, 2004.

Silvia Bucci, Mohammad Reza Loghmani, and Tatiana Tommasi. On the effectiveness of image rotation for open set domain adaptation. In *ECCV*, pp. 422–438, 2020.

Qi Dou, Daniel Coelho de Castro, Konstantinos Kamnitsas, and Ben Glocker. Domain generalization via model-agnostic learning of semantic features. In *Advances in Neural Information Processing Systems*, volume 32, pp. 6450–6461, 2019.

Yingjun Du, Jun Xu, Huan Xiong, Qiang Qiu, Xiantong Zhen, Cees GM Snoek, and Ling Shao. Learning to learn with variational information bottleneck for domain generalization. In *European Conference on Computer Vision*, pp. 200–216. Springer, 2020.

Xinjie Fan, Qifei Wang, Junjie Ke, Feng Yang, Boqing Gong, and Mingyuan Zhou. Adversarially adaptive normalization for single domain generalization. In *Proceedings of the IEEE/CVF Conference on Computer Vision and Pattern Recognition*, pp. 8208–8217, 2021.

Bo Fu, Zhangjie Cao, Mingsheng Long, and Jianmin Wang. Learning to detect open classes for universal domain adaptation. In *European Conference on Computer Vision*, pp. 567–583. Springer, 2020.

Yaroslav Ganin and Victor Lempitsky. Unsupervised domain adaptation by backpropagation. In *International conference on machine learning*, pp. 1180–1189. PMLR, 2015.

Chuanxing Geng, Sheng-jun Huang, and Songcan Chen. Recent advances in open set recognition: A survey. *IEEE transactions on pattern analysis and machine intelligence*, 2020.

Boqing Gong, Yuan Shi, Fei Sha, and Kristen Grauman. Geodesic flow kernel for unsupervised domain adaptation. In *2012 IEEE conference on computer vision and pattern recognition*, pp. 2066–2073. IEEE, 2012.

Kaiming He, Xiangyu Zhang, Shaoqing Ren, and Jian Sun. Deep residual learning for image recognition. In *Proceedings of the IEEE conference on computer vision and pattern recognition*, pp. 770–778, 2016.

Dan Hendrycks and Thomas Dietterich. Benchmarking neural network robustness to common corruptions and perturbations. In *International Conference on Learning Representations*, 2019.

Jonathan J. Hull. A database for handwritten text recognition research. *IEEE Transactions on pattern analysis and machine intelligence*, 16(5):550–554, 1994.

Vladimir Koltchinskii. *Oracle Inequalities in Empirical Risk Minimization and Sparse Recovery Problems: Ecole d'Eté de Probabilités de Saint-Flour XXXVIII-2008*, volume 2033. Springer Science & Business Media, 2011.

Samuli Laine and Timo Aila. Temporal ensembling for semi-supervised learning. In *ICLR*, 2017.

Yann LeCun, Bernhard Boser, John S Denker, Donnie Henderson, Richard E Howard, Wayne Hubbard, and Lawrence D Jackel. Backpropagation applied to handwritten zip code recognition. *Neural computation*, 1(4):541–551, 1989.

Da Li, Yongxin Yang, Yi-Zhe Song, and Timothy M Hospedales. Deeper, broader and artier domain generalization. In *Proceedings of the IEEE international conference on computer vision*, pp. 5542–5550, 2017.

Da Li, Yongxin Yang, Yi-Zhe Song, and Timothy M Hospedales. Learning to generalize: Meta-learning for domain generalization. In *Thirty-Second AAAI Conference on Artificial Intelligence*, 2018.

Hong Liu, Zhangjie Cao, Mingsheng Long, Jianmin Wang, and Qiang Yang. Separate to adapt: Open set domain adaptation via progressive separation. In *Proceedings of the IEEE/CVF Conference on Computer Vision and Pattern Recognition*, pp. 2927–2936, 2019.

Mingsheng Long, Zhangjie Cao, Jianmin Wang, and Michael I Jordan. Conditional adversarial domain adaptation. In *Proceedings of the 32nd International Conference on Neural Information Processing Systems*, pp. 1647–1657, 2018.

Krikamol Muandet, David Balduzzi, and Bernhard Schölkopf. Domain generalization via invariant feature representation. In *International Conference on Machine Learning*, pp. 10–18. PMLR, 2013.

Yuval Netzer, Tao Wang, Adam Coates, Alessandro Bissacco, Bo Wu, and Andrew Y Ng. Reading digits in natural images with unsupervised feature learning. 2011.

Shreyas Padhy, Zachary Nado, Jie Ren, Jeremiah Liu, Jasper Snoek, and Balaji Lakshminarayanan. Revisiting one-vs-all classifiers for predictive uncertainty and out-of-distribution detection in neural networks. *arXiv preprint arXiv:2007.05134*, 2020.

Pau Panareda Busto and Juergen Gall. Open set domain adaptation. In *Proceedings of the IEEE International Conference on Computer Vision*, pp. 754–763, 2017.

Xingchao Peng, Zijun Huang, Yizhe Zhu, and Kate Saenko. Federated adversarial domain adaptation. In *International Conference on Learning Representations*, 2020.

Fengchun Qiao, Long Zhao, and Xi Peng. Learning to learn single domain generalization. In *Proceedings of the IEEE/CVF Conference on Computer Vision and Pattern Recognition*, pp. 12556–12565, 2020.

Benjamin Recht, Rebecca Roelofs, Ludwig Schmidt, and Vaishaal Shankar. Do imagenet classifiers generalize to imagenet? In *International Conference on Machine Learning*, pp. 5389–5400. PMLR, 2019.

Kate Saenko, Brian Kulis, Mario Fritz, and Trevor Darrell. Adapting visual category models to new domains. In *ECCV*, pp. 213–226. Springer, 2010.

Kuniaki Saito and Kate Saenko. Ovanet: One-vs-all network for universal domain adaptation. In *ICCV*, 2021.

Kuniaki Saito, Shohei Yamamoto, Yoshitaka Ushiku, and Tatsuya Harada. Open set domain adaptation by backpropagation. In *OSDA*, pp. 153–168, 2018.

Kuniaki Saito, Donghyun Kim, Stan Sclaroff, and Kate Saenko. Universal domain adaptation through self supervision. *Advances in Neural Information Processing Systems*, 33, 2020.

Mehdi Sajjadi, Mehran Javanmardi, and Tolga Tasdizen. Regularization with stochastic transformations and perturbations for deep semi-supervised learning. In *Advances in neural information processing systems*, volume 29, pp. 1163–1171, 2016.

Shiv Shankar, Vihari Piratla, Soumen Chakrabarti, Siddhartha Chaudhuri, Preethi Jyothi, and Sunita Sarawagi. Generalizing across domains via cross-gradient training. In *ICLR*, 2018.

Yang Shu, Zhangjie Cao, Chenyu Wang, Jianmin Wang, and Mingsheng Long. Open domain generalization with domain-augmented meta-learning. In *Proceedings of the IEEE/CVF Conference on Computer Vision and Pattern Recognition*, pp. 9624–9633, 2021.

Aman Sinha, Hongseok Namkoong, and John Duchi. Certifying some distributional robustness with principled adversarial training. In *International Conference on Learning Representations*, 2018.

Vivienne Sze, Yu-Hsin Chen, Tien-Ju Yang, and Joel S Emer. Efficient processing of deep neural networks: A tutorial and survey. *Proceedings of the IEEE*, 105(12):2295–2329, 2017.

Vladimir Vapnik. Principles of risk minimization for learning theory. In *Advances in neural information processing systems*, pp. 831–838, 1992.

Hemanth Venkateswara, Jose Eusebio, Shayok Chakraborty, and Sethuraman Panchanathan. Deep hashing network for unsupervised domain adaptation. In *CVPR*, pp. 5018–5027, 2017.

Riccardo Volpi, Hongseok Namkoong, Ozan Sener, John C Duchi, Vittorio Murino, and Silvio Savarese. Generalizing to unseen domains via adversarial data augmentation. In *NeurIPS*, 2018.

Kaichao You, Mingsheng Long, Zhangjie Cao, Jianmin Wang, and Michael I Jordan. Universal domain adaptation. In *Proceedings of the IEEE/CVF conference on computer vision and pattern recognition*, pp. 2720–2729, 2019.

Sergey Zagoruyko and Nikos Komodakis. Wide residual networks. In *British Machine Vision Conference 2016*. British Machine Vision Association, 2016.

Long Zhao, Ting Liu, Xi Peng, and Dimitris Metaxas. Maximum-entropy adversarial data augmentation for improved generalization and robustness. In *NeurIPS2020*, 2020a.

Shanshan Zhao, Mingming Gong, Tongliang Liu, Huan Fu, and Dacheng Tao. Domain generalization via entropy regularization. In *Advances in Neural Information Processing Systems*, volume 33, 2020b.

Kaiyang Zhou, Yongxin Yang, Timothy Hospedales, and Tao Xiang. Learning to generate novel domains for domain generalization. In *European Conference on Computer Vision*, pp. 561–578. Springer, 2020.

Kaiyang Zhou, Ziwei Liu, Yu Qiao, Tao Xiang, and Chen Change Loy. Domain generalization: A survey. *arXiv preprint arXiv:2103.02503*, 2021a.

Kaiyang Zhou, Yongxin Yang, Yu Qiao, and Tao Xiang. Domain generalization with mixstyle. In *International Conference on Learning Representations*, 2021b.

A APPENDIX

The appendix provides descriptions of algorithm, details for datasets and experimental settings, and additional experimental results.

A.1 ALGORITHM

Algorithm 1 illustrates details of our proposed method.

Algorithm 1 CrossMatch with Adversarial Data Augmentation based Single Domain Generalization methods.

Input: Source domain $\mathcal{D}_s = \{(x_s^i, y_s^i)\}_{i=1}^{n_s}$ and generated auxiliary unknown class domain $\mathcal{D}_u = \{\}$. Initialized parameters θ_g, θ_f and θ_{f_b} for feature extractor G, multi-class classifier F and multi-binary classifier F_b.

Output: Learned feature extractor G and multi-class classifier F;

for $k = 1$ to K **do** ▷ Run the maximizing procedure K times
  for $t = 1$ to T_{MIN} **do** ▷ Run the minimization stage T_{MIN} times
    Sample (x_s, y_s) uniformly from $\mathcal{D}_s$
    $(\theta_g, \theta_f) \leftarrow (\theta_g, \theta_f) - \beta \nabla_{(\theta_g, \theta_f)} \mathcal{L}_{ce}(\theta_g, \theta_f; x_s, y_s)$
    $(\theta_g, \theta_{f_b}) \leftarrow (\theta_g, \theta_{f_b}) - \beta \nabla_{(\theta_g, \theta_{f_b})} \mathcal{L}_{ova}(\theta_g, \theta_{f_b}; x_s, y_s)$
    if $\mathcal{D}_k$ is not empty **then**
      Sample x_u uniformly from $\mathcal{D}_u$
      $(\theta_g, \theta_{f_b}) \leftarrow (\theta_g, \theta_{f_b}) - \beta \nabla_{(\theta_g, \theta_{f_b})} \mathcal{L}_{ent}^b(\theta_g, \theta_{f_b}; x_u)$
      $(\theta_g, \theta_f, \theta_{f_b}) \leftarrow (\theta_g, \theta_f, \theta_{f_b}) - \beta \nabla_{(\theta_g, \theta_f, \theta_{f_b})} \mathcal{L}_{ccr}(\theta_g, \theta_f, \theta_{f_b}; x_u)$
    end if
  end for
  for all $(x_s, y_s) \in \mathcal{D}_s$ **do**
    $x_k \leftarrow x_s$ and $x_u \leftarrow x_s$
    for $t = 1$ to T_{MAX} **do** ▷ Run the maximization stage T_{MAX} times
      $x_k \leftarrow x_k + \eta \nabla_{x_k} \{\mathcal{L}_{sdg} - \gamma \mathcal{L}_{const}(x_k, x_s)\}$
      $x_u \leftarrow x_u + \eta \nabla_{x_u} \{\mathcal{L}_{unk} + \gamma \mathcal{L}_{const}(x_u, x_s)\}$
      Append (x_k, y_s) to $\mathcal{D}_s$ and x_u to $\mathcal{D}_u$
    end for
  end for
end for
while not reach maximum steps T **do**
  Sample (x_s, y_s) uniformly from $\mathcal{D}_s$
  Sample x_u uniformly from $\mathcal{D}_u$
  $(\theta_g, \theta_f) \leftarrow (\theta_g, \theta_f) - \beta \nabla_{(\theta_g, \theta_f)} \mathcal{L}_{ce}(\theta_g, \theta_f; x_s, y_s)$
  $(\theta_g, \theta_{f_b}) \leftarrow (\theta_g, \theta_{f_b}) - \beta \nabla_{(\theta_g, \theta_{f_b})} \mathcal{L}_{ova}(\theta_g, \theta_{f_b}; x_s, y_s)$
  $(\theta_g, \theta_{f_b}) \leftarrow (\theta_g, \theta_{f_b}) - \beta \nabla_{(\theta_g, \theta_{f_b})} \mathcal{L}_{ent}^b(\theta_g, \theta_{f_b}; x_u)$
  $(\theta_g, \theta_f, \theta_{f_b}) \leftarrow (\theta_g, \theta_f, \theta_{f_b}) - \beta \nabla_{(\theta_g, \theta_f, \theta_{f_b})} \mathcal{L}_{ccr}(\theta_g, \theta_f, \theta_{f_b}; x_u)$
end while

A.2 DATASETS

Digits consists of 5 different datasets: MNIST (LeCun et al., 1989), SVHN (Netzer et al., 2011), USPS (Hull, 1994), SYN and MNIST-M (Ganin & Lempitsky, 2015). Following the setting defined by (Volpi et al., 2018; Zhao et al., 2020a), we select 10,000 images from MNIST as the source domain and the rest datasets are viewed as target domains. The source label space $\mathcal{C}_s$ contains numbers from zero to four and target unknow class space $\mathcal{C}_t^u$ includes numbers from five to nine. We resize all the images to 32×32 and duplicate their channels to convert all the grayscale images to RGB.

Office31 (Saenko et al., 2010) includes 4,652 images in 31 categories collected from three domains: Amazon (A), Webcam (W) and DSLR (D). We follow the protocol proposed by (Panareda Busto & Gall, 2017). We use the 10 classes (back pack, bike, calculator, headphones, keyboard, laptop,

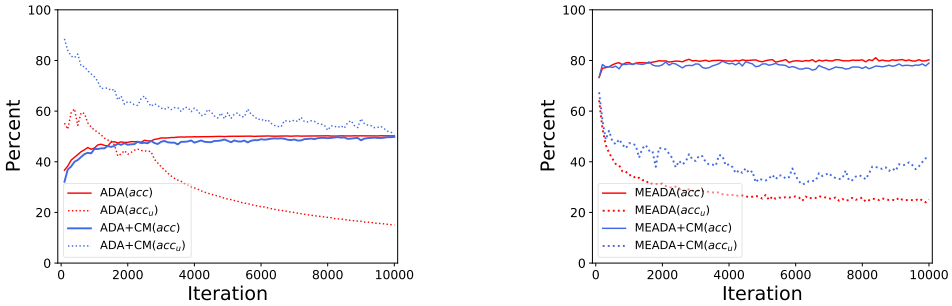

(a) (b)

Figure 5: (a) acc and acc_u convergence of ADA and ours on *Digits*. (b) acc and acc_u convergence of MEADA and ours on *Office31*.

Table 6: Results (%) on *Digits* (ConvNet) under different values of α.

α		0.4	0.6	0.8	1.0	1.2	1.4	1.6
ADA+CM	acc	49.65	50.6	49.56	49.71	49.18	50.18	48.64
	acc_u	49.69	51.56	47.53	52.07	52.36	48.14	56.62
	hs	38.44	41.04	38.54	39.93	39.6	39.13	40.81
MEADA+CM	acc	50.65	52.3	51.6	51.27	51.57	50.47	51.01
	acc_u	46.66	37.78	42.53	46.11	42.29	51.53	48.02
	hs	39.14	36.34	37.07	38.70	37.36	41.67	40.08

monitor, mouse, mug and projector) shared by Office-31 and Caltech-256 (Gong et al., 2012) as the source domain label space $\mathcal{C}_s$. Then in alphabetical order, the last 11 classes (ruler, punchers, stapler, scissors, trash can, tape dispenser, pen, phone, printer, ring binder and speaker) are used as target unknown class space $\mathcal{C}_t^u$. Due to the number of images in DSLR and Webcam are relatively small, we only use Amazon as the source domain.

Office-Home (Venkateswara et al., 2017) contains 15,500 images from four domains: Artistic (Ar), Clip Art (Cl), Product (Pr), and Real-World (Rw). As it comprises of 65 categories from four dissimilar domains, it's more challenging than *Digits* and *Office-31*. In alphabetic order, we select the first 15 classes (alarm clock, backpack, battery, bed, bike, bottle, bucket, calculator, calendar, candles, chair, clipboards, computer, couch and curtains) as the source label space $\mathcal{C}_s$. The remaining 50 classes are viewed as target unknown label space $\mathcal{C}_t^u$. Each time, one domain is selected as source domain and the rest are viewed as target domain.

PACS (Li et al., 2017) is a recent challenging benchmark for domain generalization that includes four domains: Art Paint, Cartoon, Sketch, and Photo. It consists of 9,991 images and seven object categories shared across these domains. In alphabetic order, we choose the first four classes (dog, elephant, giraffe, and guitar.) as the source label space $\mathcal{C}_s$. The last three classes (horse, house, and person.) are selected as target unknown label space $\mathcal{C}_t^u$. We train the model by one domain and evaluate the learned model by the rest domains

A.3 Evaluation Metrics.

We adopt the evaluation protocol in Open-Set Domain Adaptation (Panareda Busto & Gall, 2017), where all the target classes out of $\mathcal{C}_s$ are regarded as one unified unknown class. We compute the mean accuracy averaged over all classes in $|\mathcal{C}_s| + 1$ (i.e., acc) and the unknown class accuracy (i.e., acc_u) across all target domains. To better evaluate the capability of methods on unknown class identification, we also adopt the *h-score* (*hs*) (Fu et al., 2020) metric, $hs = 2 * acc_s * acc_u/(acc_s + acc_u)$. It is the harmonic mean of average per-class accuracy in $\mathcal{C}_s$ (i.e., acc_s) and acc_u. The *h-score* value is high only when both acc_s and acc_u are high.

Table 7: Results (%) on *Digits* (ConvNet) under different values of μ.

Metric	μ=0.2		μ=0.6		μ=0.804		μ=1.0		μ=1.2	
	ERM	*ERM+CM*	*ERM*	*ERM+CM*	*ERM*	*ERM+CM*	*ERM*	*ERM+CM*	*ERM*	*ERM+CM*
acc_s	48.54	42.34	54.07	48.36	56.40	48.67	58.13	53.68	58.98	56.35
acc_u	47.25	69.61	25.21	53.91	13.04	53.52	5.91	38.17	1.66	29.36
acc	48.37	46.88	49.26	49.28	49.17	49.07	49.42	51.09	48.02	51.85
hs	40.82	42.68	29.69	40.28	17.97	40.15	9.77	33.88	3.09	28.98

Table 8: Known classes accuracy (%) and unknown class accuracy (%) on *Office-Home* (ResNet18).

Method	Artistic		Clip Art		Product		Real-World		Average	
	acc_s	acc_u	acc_s	acc_u	acc_s	acc_u	acc_s	acc_u	acc_s	acc_u
OSDAP	44.13	67.84	51.69	69.26	40.00	63.47	52.48	66.92	47.07	66.87
OpenMax	17.38	98.08	17.72	97.04	9.53	98.59	20.78	97.01	16.35	97.68
ERM	68.54	20.53	66.75	24.65	62.81	26.26	69.48	23.18	66.90	23.66
ERM+CM	66.48	48.57	64.80	41.95	59.17	40.94	69.36	43.69	64.95	**43.79**
ADA	71.36	22.05	67.37	31.19	62.91	24.55	69.92	23.88	67.89	25.42
ADA+CM	67.53	39.59	64.10	40.67	59.92	40.72	68.53	40.79	65.02	**40.44**
MEADA	71.37	22.36	66.45	31.27	62.75	25.60	69.92	23.71	67.62	25.74
MEADA+CM	66.63	45.28	64.43	37.84	59.74	37.71	68.82	41.28	64.90	**40.53**

A.4 Implementation Details

We set the same parameters and optimization functions to baselines and ours.

Digits. Following the setup of (Volpi et al., 2018; Zhao et al., 2020a). We use ConvNet (LeCun et al., 1989) (*conv-pool-conv-pool-fc-fc-softmax*) as the base model. The batch size is 32. We adopt Adam with learning rate $\beta = 0.0001$ for minimization stage and SGD with learning rate $\eta = 1.0$ for maximization stage. We set $T = 10000$, $T_{MIN} = 100$, $T_{MAX} = 15$, $K = 3$, $\gamma = 1.0$ and $\alpha = 1$. The reported results are the averaged results based on 10 random experiments.

Office31, Office-Home and PACS. Referring to the setup of (Zhao et al., 2020a) on *PACS*, we adopt ImageNet-pretrained ResNet18 as base network and set the batch size to 32. We use SGD with learning rate $\beta = 0.001$ which adjusted by a cosine annealing schedule (Zagoruyko & Komodakis, 2016), the momentum of 0.9 and the weight decay of 0.00005 for minimization stage. We adopt the SGD with learning $\eta = 1.0$ for maximization stage. We set $T = 10000$, $T_{MIN} = 100$, $T_{MAX} = 15$, $K = 1$, $\gamma = 1.0$ and $\alpha = 1$. The reported results are the averaged results based on 3 random experiments.

A.5 Convergence Analysis

We testify the convergence performance of our method under acc and acc_u by comparing it against ADA and MEAD on the *Digits* and *Office31* datasets. Figure 5(b) and (c) illustrate the capability of our method on improving the unknown class identification performance. We observe that the value of acc_u is relatively high at the early training stage. This phenomenon is induced by the model that is not well-trained and prefers to output high entropy values for testing samples. Even though the performance of acc_u drops during the training process, our method still outperforms ADA and MEADA in terms of acc_u while achieving similar mean accuracy acc.

A.6 Parameter Sensitivity

We analyze the sensitivity of α in Eq. 8 on *Digits* datasets by varying it from 0.4 to 1.6. Table 6 shows performance of our method in terms of acc, acc_u, and hs. Compared ADA and MEADA performance on *Digits* datasets (in Table 2), our method significantly outperforms them with respect to acc_u and hs while obtains comparable results on acc, which proves our method is robust to different choices of

Table 9: Known classes accuracy (%) and unknown class accuracy (%) on *PACS* (ResNet18).

Method	Art Paint		Cartoon		Sketch		Photo		Average	
	acc_s	acc_u	acc_s	acc_u	acc_s	acc_u	acc_s	acc_u	acc_s	acc_u
OSDAP	54.17	49.84	41.36	51.68	38.84	54.92	28.09	41.62	40.62	49.51
OpenMax	42.87	91.48	15.27	97.44	13.16	96.61	11.96	90.22	20.82	93.94
ERM	68.80	24.57	59.46	33.08	43.34	20.27	37.54	30.03	52.29	26.99
ERM+CM	68.66	44.56	62.25	43.18	41.01	33.16	39.91	54.21	**52.96**	**44.53**
ADA	70.95	28.80	62.08	33.83	43.18	22.41	40.65	38.77	54.22	30.93
ADA+CM	72.93	40.12	64.39	49.06	44.98	40.85	43.27	52.53	**56.40**	**45.64**
MEADA	70.90	28.65	62.09	33.55	43.42	22.90	39.78	40.31	54.05	31.35
MEADA+CM	70.45	33.36	63.76	53.74	40.25	48.79	42.89	50.57	**54.34**	**46.61**

Table 10: Results (%) with STD Value on *Digits* (ConvNet) and *Office31* (ResNet18).

		ERM	ERM+CM	ADA	ADA+CM	MEADA	MEADA+CM
Digits	*acc*	49.17±0.2	49.07±0.2	50.22±0.1	49.71±0.2	52.98±0.2	51.27±0.1
	acc_u	13.04±0.1	**53.52**±0.1	15.11±0.2	**52.07**±0.3	29.83±0.2	**46.11**±0.2
	acc_s	56.40±0.2	48.67±0.2	57.24±0.3	49.24±0.2	57.61±0.3	52.30±0.2
	hs	17.97±0.2	**40.15**±0.1	20.14±0.2	**39.93**±0.2	30.37±0.2	**38.70**±0.2
Office31	*acc*	79.82±0.3	78.30±0.3	80.13±0.2	78.61±0.2	80.26±0.2	78.98±0.2
	acc_u	27.04±0.5	**37.60**±0.2	25.24±0.3	**34.51**±0.3	25.09±0.3	**41.08** ±0.2
	acc_s	85.10±0.2	82.37±0.2	85.62±0.3	83.02±0.3	85.78±0.3	82.77±0.3
	hs	40.69±0.4	**51.14**±0.2	38.65±0.3	**48.50**±0.3	38.55±0.2	**54.69**±0.2

α. We also evaluate the sensitivity of μ in Figure 3 on *Digits*. As shown in Table 7, With small value of μ, the inference framework would mark many known classes samples as unknown class. With large value of μ, the inference framework will reject many unknown class samples to known classes.

A.7 Performance of Unknown Class Identification and Known Classes Classification

We report the performance of our method and baselines in terms of unknown class accuracy acc_u and known classes accuracy acc_s on *Office-Home* and *PACS* datasets. More details can be found in Table 8 and 9.

A.8 Experimental Results with Standard Deviation (STD)

We provide STD value for our method and baselines, i.e., ERM, ADA, and MEADA on four datasets, i.e., *Digits*, *Office31*, *Office-Home*, and *PACS* in Table 10, 11, and 12.

Table 11: Results (%) with STD value on *Office-Home* (ResNet18).

Method	Artistic		Clip Art		Product		Real-World		Average	
	acc	*hs*	*acc*	*hs*	*acc*	*hs*	*acc*	*hs*	*acc*	*hs*
ERM	65.00±0.3	31.07±0.6	64.12±0.3	35.78±0.6	60.53±0.4	36.33±0.5	66.59±0.3	33.92±0.5	64.06	34.28
ERM+CM	65.49±0.3	52.85±0.4	63.37±0.4	50.51±0.6	58.03±0.3	47.25±0.7	67.75±0.6	52.60±0.4	63.66	**50.80**
ADA	68.29±0.6	32.94±0.4	65.10±0.4	42.09±0.3	60.52±0.2	34.72±0.3	67.04±0.3	34.86±0.4	65.24	36.15
ADA+CM	66.30±0.4	46.68±0.3	62.64±0.5	49.31±0.4	58.72±0.3	47.47±0.3	66.82±0.4	50.47±0.3	63.62	**48.48**
MEADA	68.31±0.3	33.29±0.4	65.25±0.4	42.05±0.5	60.43±0.3	35.68±0.2	67.04±0.3	34.65±0.4	65.01	36.42
MEADA+CM	65.85±0.4	53.22±0.4	62.90±0.3	48.87±0.2	58.36±0.3	45.34±0.3	67.10±0.2	50.77±0.3	63.55	**49.55**

Table 12: Results (%) on *PACS* (ResNet18).

Method	Art Paint		Cartoon		Sketch		Photo		Average	
	acc	*hs*	*acc*	*hs*	*acc*	*hs*	*acc*	*hs*	*acc*	*hs*
ERM	62.24±0.5	38.90±0.4	55.34±0.6	40.96±0.5	39.19±0.4	28.89±0.3	38.32±0.2	35.74±0.4	48.77	36.12
ERM+CM	63.52±0.4	44.9±0.6	57.6±0.4	48.31±0.5	38.53±0.5	30.43±0.6	42.52±0.3	41.6±0.4	**50.54**	**41.31**
ADA	62.48±0.6	39.02±0.4	56.43±0.4	41.55±0.5	39.03±0.2	26.93±0.4	40.28±0.6	38.13±0.5	49.56	36.41
ADA+CM	64.26±0.5	42.4±0.6	60.41±0.4	51.81±0.4	42.48±0.3	35.18±0.5	43.97±0.4	42.76±0.7	**52.78**	**43.04**
MEADA	62.43±0.4	38.85±0.3	56.1±0.6	41.34±0.4	38.89±0.7	26.43±0.5	39.88±0.6	38.24±0.4	49.33	36.22
MEADA+CM	62.63±0.5	41.88±0.6	60.03±0.3	51.36±0.6	41.51±0.4	35.76±0.4	43.5±0.5	41.6±0.5	**51.92**	**42.65**